Submitted: 23 October, 2023 Accepted: 05 January, 2024 Published: 15 April, 2024 DOI:10.22514/ejgo.2024.023

ORIGINAL RESEARCH

European Journal of Gynaecological Oncology

Predictive value of multimodal ultrasound imaging and BCL-2 expression levels in the outcome of neoadjuvant chemotherapy for breast cancer

Xueqin Hou[1], Junxi Gao[1], Yibin Liu[1], Wei Han[1], Zhiming Li[1], Tao Song[1,*]

[1]Department of Abdominal Ultrasound Diagnosis, The First Affiliated Hospital of Xinjiang Medical University, Xinjiang Key Laboratory of Ultrasound Medicine, 830054 Urumqi, Xinjiang Uygur Autonomous Region, China

***Correspondence**
tsong8987@163.com
(Tao Song)

Abstract

A cohort of 60 breast cancer patients undergoing neoadjuvant chemotherapy (NAC) from January 2021 to December 2022 was studied at the First Affiliated Hospital of Xinjiang Medical University. Multimodal ultrasound examinations were conducted before and after NAC. Levels of B-lymphocytoma-2 (BCL-2) and Ki-67 were assessed through immunohistochemistry both before NAC and during radical mastectomy. Based on the Miller-Payne system, the efficacy of NAC in these patients was categorized into pathologic complete remission (pCR) and non-complete remission (npCR). It was found that: Pathological evaluation postoperatively revealed that 26 patients achieved pCR, while 34 experienced npCR following NAC. In both pCR and npCR groups, significant reductions in lesion diameter, peak intensity (PI), area under the curve (AUC) and elasticity score were observed post-NAC, as well as an increase in Strain Ratio (SR). These changes were more pronounced in the pCR group, with statistically significant differences ($p < 0.05$). Post-NAC, an increase in BCL-2 and a decrease in Ki-67 expression were observed in both groups, although these changes were not statistically significant ($p > 0.05$). Receiver operating characteristic (ROC) curves and multifactorial regression analysis identified lesion diameter, PI and AUC as significant predictors of NAC efficacy in breast cancer patients.

Keywords

Breast cancer; Neoadjuvant chemotherapy; Multimodal ultrasound; BCL-2; Complete remission; ROC curves

1. Introduction

Breast cancer, a prevalent malignancy among females, poses a significant threat to women's lives. Neoadjuvant chemotherapy (NAC) has demonstrated effectiveness in increasing surgical resection rate and breast conservation rate in locally advanced breast cancer. It also diminishes the risk of postoperative tumor recurrence and metastasis, ultimately improving patient prognosis [1–3]. Presently, NAC has become the standard therapeutic approach for locally advanced breast cancer [4, 5]. Precise assessment of NAC's effectiveness is an important prerequisite for formulating subsequent treatment strategies. While pathological tissue biopsy is considered the "gold standard" for assessing the effectiveness of NAC, it is typically performed after surgery, which introduces a time delay [6].

Ultrasound is the most common method for breast cancer screening. Advances in ultrasound technology have led to studies advocating the integration of multimodal ultrasound into clinical practice, offering additional insights into the assessment of NAC efficacy in breast cancer management [7, 8]. Furthermore, a significant association exists between BCL-2 expression and breast cancer. Thus, assessing BCL-2 expression levels in cancerous tissues could improve the prediction of NAC efficacy [9]. Thus, this study aims to investigate the predictive value of multimodal ultrasound imaging with BCL-2 expression analysis in assessing NAC outcomes among breast cancer patients.

2. Materials and methods

2.1 Study participants

A total of 60 breast cancer patients who underwent NAC at the First Affiliated Hospital of Xinjiang Medical University between January 2021 and December 2022 were enrolled in this study.

The study inclusion criteria encompassed patients who had a confirmed breast cancer diagnosis through puncture biopsy, a clinical diagnosis of stage II or III breast cancer based on clinical examination and relevant adjuvant tests, underwent surgical intervention followed by 4 weeks of NAC therapy, and were willing to actively participate in the pathological examination, multimodality ultrasound, and BCL-2 analysis.

Conversely, the exclusion criteria comprised patients diagnosed with metastatic breast cancer, those presenting with multiple lesions, individuals with known allergies to contrast agents, patients affected by severe cardiopulmonary diseases, and those who demonstrated intolerance to NAC or displayed poor chemotherapy compliance.

After screening, a cohort of 60 breast cancer patients, aged 45 to 66 years, with an average age of (51.34 $\pm$ 12.35) years and a weight range of 42 to 67 kg, averaging (61.15 $\pm$ 3.45) kg, were found eligible. Tumor staging data analysis indicated that there were 31 cases classified as stage II and 29 cases as stage III. In addition, we identified 43 cases of invasive ductal carcinoma, 12 cases of invasive lobular carcinoma, and 5 cases of medullary carcinoma. Lymph node metastasis was observed in 13 cases, while no evidence of distant metastasis was detected in any of the included cases.

2.2 Multimodal ultrasound examination

2.2.1 Examination instruments and reagents

The diagnostic instruments utilized in this study comprised the LOGIQ E9 color Doppler ultrasound system (GE), equipped with L9 and L15 high-frequency linear array probes with a frequency range of 9 to 15 MHz. Additionally, we used the AIXPLORERV ultrasound diagnostic instrument (AIXPLORERV, Aix-en-provence, France, SuperSonic Imaginer), which was equipped with an L15 high-frequency linear array probe offering a frequency range of 4 to 15 MHz. The contrast agent utilized was obtained from Bracco.

2.2.2 Examination methods

Conventional Ultrasound Examination: For routine ultrasound examination, the LOGIQ E9 color Doppler ultrasound was used. Initially, we selected the L15 probe to conduct a thorough scan of both breasts and axillary regions, and upon identifying suspicious lesions, multiplanar and multi-angle scans were performed. We recorded the maximum diameter of the lesion and assessed aspects such as the lesion's boundary, internal blood flow, and resistance index (RI).

Contrast-Enhanced Ultrasound Examination (CEUS): To perform this examination, we utilized the LOGIQ E9 color Doppler ultrasound diagnostic instrument. Initially, we positioned the L9 probe to obtain the largest cross-sectional view of the lesion, then switched to the dual-screen breast imaging mode, maintaining a fixed mechanical index of 0.04. Next, the contrast agent SonoVue suspension (4.8 mL) was introduced through the peripheral cubital vein, followed by a 5 mL saline flush through the pipeline. We activated the dynamic storage timer and adjusted the probe position to observe enhancement in various planes. The characteristics of the enhancement, including enhancement mode, intensity, uniformity, boundary clarity, and the presence of perfusion defect areas, were recorded. Additionally, we selected three to four points within both the central and peripheral areas of the lesion to generate the time-intensity curve (TIC). Parameters such as the upslope rate (K), peak intensity (PI), time to peak, and area under the curve (AUC) were recorded [10].

Real-Time Shear Wave Elastography (SWE): After identifying the largest cross-sectional view of the lesion, the instrument was switched to the SWE mode. The SWE image provides a representation of tissue hardness, featuring a semi-transparent color-coded overlay superimposed on the grayscale image. This color spectrum ranges from blue (indicative of soft tissue) to red (indicative of firm tissue). Then, we delineated regions of interest (ROI), and the instrument's integrated software was used to measure both the maximum elastic hardness (Emax) and the average elastic hardness (Emean) of the lesion. Subsequently, we calculated the elastic score for the lesion and determined the ratio of elastic strain rate [11].

2.3 Immunohistochemical detection of BCL-2 Levels

During surgery, breast cancer tissue specimens were collected and immediately submerged in liquid nitrogen at a temperature of -196 °C for preservation. Immunohistochemical staining was conducted to assess the expression levels of BCL-2 and Ki-67 in the tissue samples. For the evaluation of BCL-2 expression, a threshold of $\leq$10% was considered negative, while $>$10% was categorized as positive. Similarly, for Ki-67 expression assessment, a cutoff of $\leq$20% indicated a negative result, whereas $>$20% was considered positive [12].

2.4 Therapeutic assessment

The histopathological therapeutic assessment was conducted using the Miller-Payne system, which comprises five grades: G1, G2, G3, G4 and G5. Cases categorized as G3, G4 and G5 were considered to represent pathological complete response (pCR), while those classified as G1 and G2 were designated as non-pCR.

2.5 Statistical analysis

Data analysis was performed using the SPSS 22.0 statistical software (BMI Corporation, Chicago, IL, USA). Continuous variables are expressed as mean $\pm$ standard deviation ($\bar{x} \pm s$). To compare means between the two groups, the independent sample *t*-test was employed, while the paired *t*-test was used for before-and-after treatment comparisons. Categorical data are presented as counts (n) and assessed between groups using the chi-square test. Receiver Operating Characteristic (ROC) curves were generated to assess the predictive value of various indicators for NAC efficacy in breast cancer. Additionally, a binary linear regression model was applied to analyze factors influencing NAC efficacy, with statistical significance set at $p < 0.05$.

3. Results

3.1 Comparison of multimodal ultrasound before and after NAC treatment in the two groups

Postoperative pathological examination revealed that among the 60 patients, 26 cases achieved pCR, while 34 were npCR. In the pCR group, after NAC, patients exhibited reduced lesion diameter, PI, AUC, peak intensity and elasticity score compared to their pre-treatment measurements and increased in time to peak and SR. Similarly, among patients with npCR,

NAC treatment led to reduced maximum diameter of enlarged lymph nodes, PI and peak intensity, and an increase in SR, while the other indicators demonstrated no significant changes. Furthermore, changes in lesion diameter, PI, AUC, time to peak, peak intensity, SR and elasticity score were significantly more pronounced in the pCR group compared to the npCR group ($p < 0.05$, Table 1). Fig. 1 shows the multimodal ultrasound data of breast cancer patients before and after NAC treatment.

3.2 Comparison of BCL-2 and Ki-67 expression in lesions between the two groups

After NAC treatment, both pCR and npCR patients showed an increase in the rates of positive BCL-2 expression and a decrease in Ki-67 expression in their cancerous tissues compared to pre-treatment levels ($p < 0.05$, Table 2). However, no statistically significant difference was observed between the two groups both before and after treatment ($p > 0.05$, Table 2). Fig. 2 provides a visual representation of BCL-2 expression in breast cancer before and after NAC treatment.

3.3 Value of multimodal ultrasound and BCL-2 in predicting NAC efficacy in patients

The ROC curve analysis demonstrates that lesion diameter, PI, AUC, time to peak, peak intensity and elasticity score had certain significance in predicting the effectiveness of NAC in breast cancer patients (Table 3, Fig. 3).

3.4 Multifactorial regression analysis of multimodal ultrasound and BCL-2 to predict the efficacy of NAC in breast cancer

Multifactorial regression analysis revealed that lesion diameter, PI and AUC were identified as factors significantly associated with the effectiveness of NAC in breast cancer patients, as illustrated in Table 4.

4. Discussion

NAC involves administering 4–8 cycles of chemotherapy to patients with locally advanced breast cancer before surgery. It serves as a means to improve surgical resection rates, and therefore, identifying methods that can accurately evaluate NAC's efficacy and assess tumor response and sensitivity to chemotherapy are important to guide subsequent treatment planning [13–16]. Ultrasound, with its cost-effectiveness and non-invasive nature, offers distinct advantages over other modalities like MRI (magnetic resonance imaging) and X-rays. Additionally, multimodal ultrasound can comprehensively assess changes in tumor tissue before and after NAC from multiple angles, providing valuable references for subsequent treatments.

The primary criterion for evaluating the effectiveness of NAC using two-dimensional ultrasound (2D US) is the reduction in tumor size. However, some studies have shown that a significant proportion of patients initially categorized as having an inadequate response based on ultrasound evaluations were found to have actually responded positively to NAC based on postoperative pathological findings [17–19]. Thus,

TABLE 1. Comparison of multimodal ultrasound before and after NAC treatment in the two groups.

Multimodal ultrasound	pCR group			npCR group			Comparison difference value	
	Before NAC	After NAC	Difference value	Before NAC	After NAC	Difference value	*t*	*p*
Focal diameter (mm)	18.46 ± 3.11	9.15 ± 2.31[a]	9.31 ± 1.76	18.13 ± 3.25	13.59 ± 2.49[a]	4.54 ± 1.05	13.070	<0.001
Blood flow resistance index	0.79 ± 0.15	0.73 ± 0.13	--	0.81 ± 0.17	0.78 ± 0.14	--	--	--
PI	34.15 ± 3.85	22.74 ± 4.11[a]	11.41 ± 1.86	33.76 ± 3.97	31.46 ± 4.03[a]	2.30 ± 0.53	27.214	<0.001
AUC	681.15 ± 78.59	516.18 ± 80.41[a]	164.97 ± 20.79	679.79 ± 80.16	663.69 ± 74.15	16.10 ± 2.76	41.386	<0.001
K	0.14 ± 0.03	0.13 ± 0.02	--	0.12 ± 0.02	0.11 ± 0.03	--	--	--
Time to peak	22.15 ± 3.15	25.34 ± 2.45[a]	3.19 ± 0.85	21.79 ± 3.19	22.43 ± 2.63	0.64 ± 0.21	16.873	<0.001
SR	0.93 ± 0.21	2.23 ± 0.39[a]	1.31 ± 0.25	0.87 ± 0.24	1.51 ± 0.41[a]	0.64 ± 0.16	12.623	<0.001
Elasticity score	3.68 ± 0.69	2.15 ± 0.73[a]	1.53 ± 0.32	3.57 ± 0.75	3.11 ± 0.77	0.46 ± 0.11	18.183	<0.001

pCR: pathologic complete remission; npCR: non-complete remission; NAC: neoadjuvant chemotherapy; PI: peak intensity; AUC: area under the curve; K: upslope rate; SR: Strain Ratio. [a]*: Compared with NAC Before treatment, p < 0.05.*

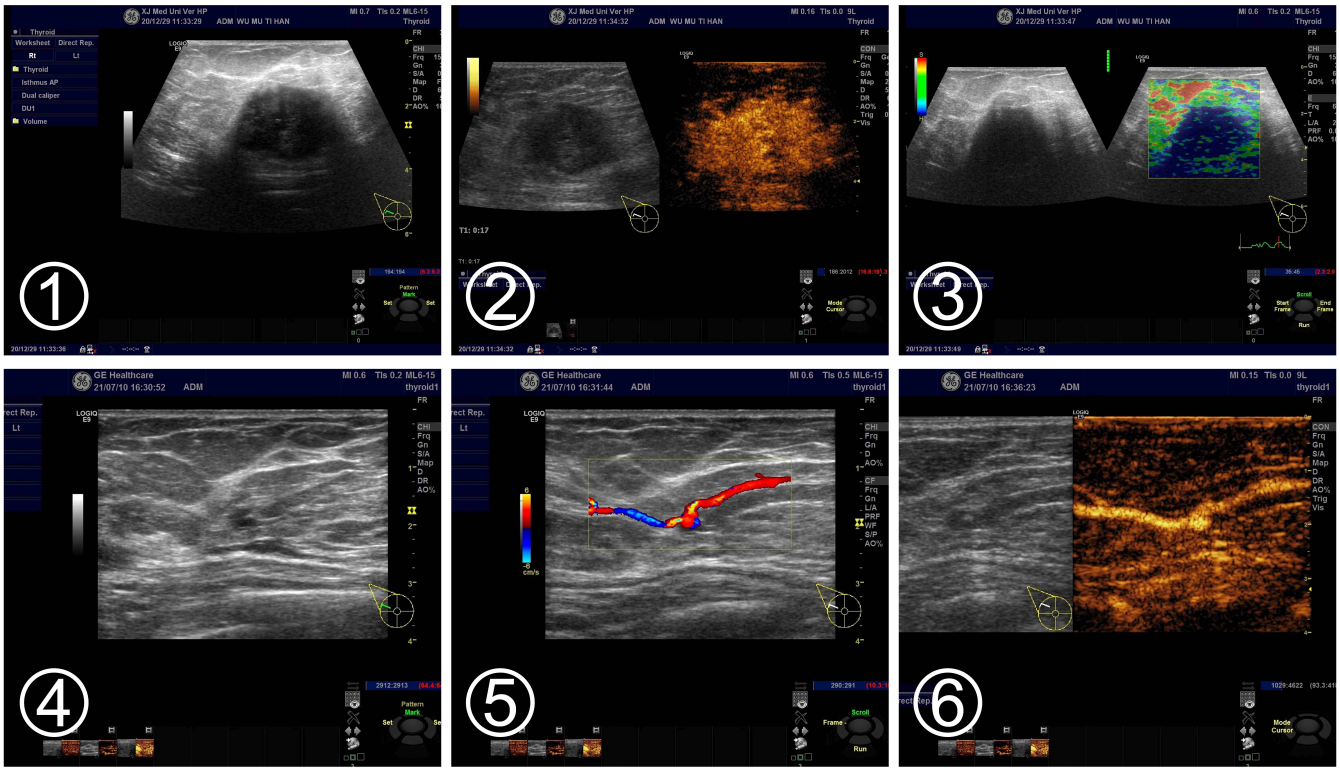

FIGURE 1. Multimodal ultrasound results before and after neoadjuvant therapy in a patient with breast cancer. ①–③ shows the results of ultrasound multimodal examination prior to NAC. A hypoechoic nodule, approximately measuring 3.2 cm × 2.4 cm × 2.8 cm, was observed in the right mammary gland between the 9 to 10 o'clock position, approximately 1.3 cm from the body surface. The nodule displayed a foliated, burr-like edge, accompanied by acoustic attenuation at the back, and exhibited heterogeneous internal echogenicity with clustered accumulations of multiple punctate strong echoes. Color Doppler Flow Imaging (CDFI) revealed striated blood flow signals both in the periphery and interior. Ultrasonography indicated rapid hyperenhancement of the nodule with subsequent slow regression. The enhancement area significantly expanded without any apparent filling defects, and a convergence sign was visible around the lesion. ④–⑥ illustrate the multimodal ultrasonography results obtained after 6 weeks of NAC treatment. In two-dimensional ultrasound, the original lesion at the edge of the gland at the 9 to 10 o'clock position in the right breast was no longer clearly visible. CDFI revealed the presence of a thick arterial vessel in the periphery, along with a local angiomatous dilatation measuring approximately 0.5 cm × 0.4 cm. Ultrasonography did not show any noticeable local abnormal enhancement.

relying solely on 2D US and changes in tumor size to assess NAC efficacy has limitations. In certain cases, NAC treatment for breast cancer results in tumor cell necrosis, leading to the formation of granulation and proliferation of fibrous tissue. Despite these changes, the tumors may still display irregular morphology and hypoechoic characteristics in ultrasound scans, causing them to be incorrectly categorized as having an ineffective NAC response [20]. Consequently, morphology-based evaluation alone cannot reliably distinguish between necrotic tumor tissue and fibrotic scars or residual tumors.

Moreover, CDFI is used to detect tumor blood flow signals. After NAC, inflammatory changes occur in the intima of blood vessels within the breast cancer tumor, resulting in vascular constriction, occlusion and reduced blood supply in the tumor. Several studies have demonstrated a decrease in blood flow grading within the tumor tissue after NAC [21]. Additionally, tumor cell necrosis can alleviate compression on peripheral blood vessels and reduce vascular resistance [22]. However, our study found no significant changes in the blood flow resistance index before and after treatment among patients with both pCR and npCR, and this lack of significant change may be attributed to the relatively small sample size in our study.

Contrast-enhanced ultrasound imaging uses the nonlinear effects of gas microbubbles in the blood to cause an intense backscattering in the acoustic field, thus yielding enhanced contrast images [23], and can be effectively used to visualize the internal blood perfusion within tumors. In this study, patients with pCR and npCR displayed decreased PI levels after NAC compared to their pre-NAC levels. Additionally, there was a slight increase in the time to peak following NAC treatment. These observations could be attributed to the anti-angiogenic effects of chemotherapy drugs, which induce changes in tumor neovascular blood flow and functionality, ultimately promoting tumor apoptosis [24]. Our study further highlights that ultrasound imaging parameters, including PI, time to peak and differences in AUC before and after NAC, hold promise in predicting the therapeutic response in breast cancer patients undergoing NAC.

TABLE 2. Comparison of BCL-2 and Ki-67 expression in lesions between the two groups (n).

Groups	Time	BCL-2	Ki-67
pCR group (n = 26)			
	Before NAC treatment	8	23
	After NAC treatment	18	13
	χ^2	7.692	9.028
	p	0.006	0.003
npCR group (n = 34)			
	Before NAC treatment	11	29
	After NAC treatment	24	20
	χ^2	9.950	5.916
	p	0.002	0.015
Comparison before treatment	χ^2/p	0.017/0.896	0.128/0.721
Comparison after treatment	χ^2/p	0.013/0.909	0.464/0.496

BCL-2: B-lymphocytoma-2; pCR: pathologic complete remission; npCR: non-complete remission; NAC: neoadjuvant chemotherapy.

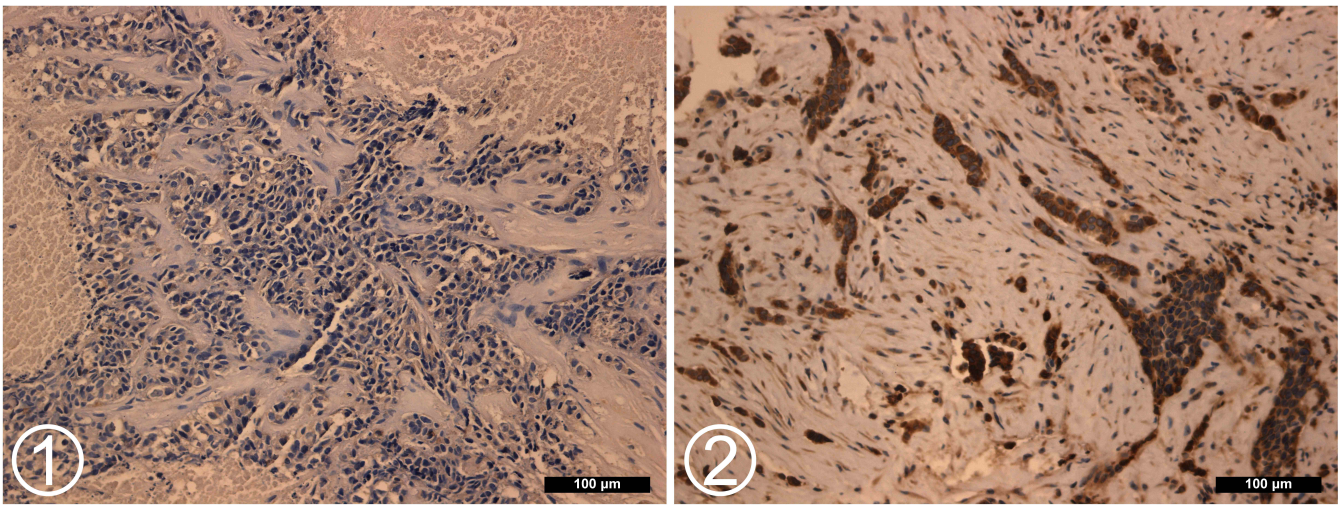

FIGURE 2. BCL-2 expression in a breast cancer patient before and after neoadjuvant therapy. ① displays BCL-2 expression before treatment, which was negative, with a BCL-2 positive expression rate of <10%. ② illustrates BCL-2 expression after treatment, which became positive, with a BCL-2 positive expression rate ranging from 10% to 25%.

TABLE 3. Significance of multimodal ultrasound and BCL-2 in predicting NAC efficacy in patients.

Indicators	Truncated value	AUC	p	95% CI
Lesion diameter	6.04	0.779	<0.001	0.654–0.904
PI (dB)	3.08	0.827	<0.001	0.723–0.932
AUC (dB·S)	118.45	0.856	<0.001	0.763–0.948
Time to peak	1.18	0.854	<0.001	0.760–0.948
SR	1.10	0.504	0.958	0.756–0.944
Elasticity score (points)	0.61	0.851	<0.001	0.344–0.642
BCL-2	--	0.570	0.074	0.425–0.716
Ki-67	--	0.535	0.644	0.388–0.682

AUC: area under the curve; CI: confidence interval; PI: peak intensity; SR: Strain Ratio; BCL-2: B-lymphocytoma-2.

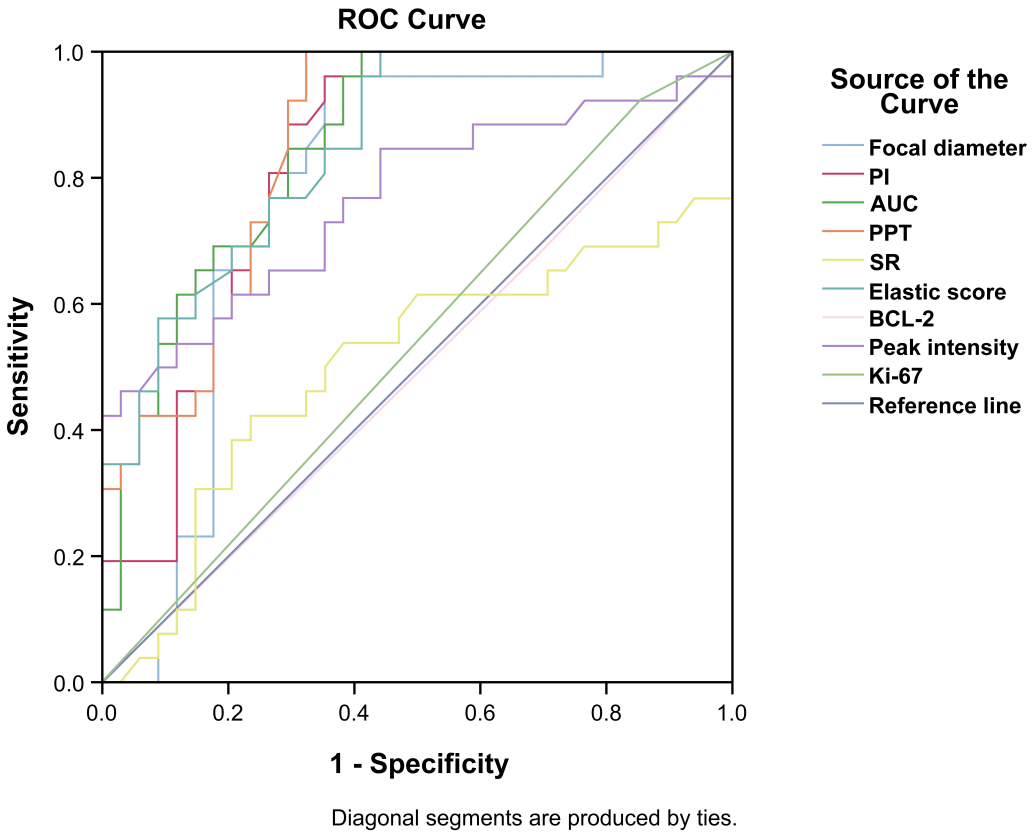

FIGURE 3. ROC curves of multimodal ultrasound and BCL-2 for predicting NAC outcomes in breast cancer patients. ROC: Receiver operating characteristic; AUC: area under the curve; PI: peak intensity; SR: Strain Ratio; BCL-2: B-lymphocytoma-2.

TABLE 4. Multifactorial regression analysis of multimodal ultrasound and BCL-2 in predicting NAC efficacy in breast cancer.

Indicators	B	Standard error	OR (95% CI)	*p* value
Lesion diameter	0.789	0.165	1.593–3.042	<0.001
PI (dB)	0.684	0.226	1.273–3.086	0.003
AUC (dB·S)	0.698	0.167	1.449–2.788	<0.001

OR: odds ratio; CI: confidence interval; PI: peak intensity; AUC: area under the curve.

Elastography is an imaging technique used to measure tissue hardness. Previous studies have established a connection between greater tissue hardness in infiltrating lesions within breast masses and an elevated risk of poor patient prognosis [25]. NAC can induce changes in both the internal and surrounding tissues of breast cancer lesions due to the effects of the drugs, leading to alterations in tissue hardness [26]. In our present study, we observed significant changes in the ultrasound elastography parameter SR before and after treatment, while only the group of patients achieving pCR had decreased elastic scores after NAC treatment. Subsequently, our ROC curve analysis indicated that SR had limited value in predicting NAC treatment outcomes, while the degree of change in elastic scores exhibited a certain level of predictive value in assessing the efficacy of NAC treatment.

Multiple factor regression analysis suggests that tumor diameter, PI and AUC were correlated factors for predicting NAC efficacy in breast cancer. Notably, ultrasound blood flow imaging parameters were not included in the regression equation due to the subtle blood flow changes in the lesion, which undergoes tissue necrosis after NAC, as well as the high level of expertise required for measuring blood flow resistance index. Thus, based on our study findings, it can be deduced that changes in tumor diameter, PI and AUC could also serve as reliable reference indicators for predicting the effectiveness of NAC in breast cancer.

With ongoing advancements in research, breast cancer has entered the era of molecular biology and genomics, and research into the relationships between various molecular biological factors and breast cancer has become a current research focus [27, 28]. BCL-2 is a broadly defined anti-apoptotic gene, and its ability to inhibit cell apoptosis is enhanced when combined with Bag-1, consequently promoting tumor cell replication and metastasis [29]. Ki-67 is a common marker that

reflects tumor proliferation status [30], where a higher positive expression rate of Ki-67 indicates stronger tumor proliferation activity [31]. In this study, we observed that after NAC, the positive expression rates of BCL-2 increased in breast cancer lesions, while the rates of Ki-67 decreased. However, neither of these factors demonstrated strong predictive efficacy for assessing the effectiveness of NAC. This observation may be associated with the bias introduced by the relatively small sample size included in this study. Nevertheless, it is important to acknowledge that the limited sample size and the single-center nature of the study might have also introduced certain level of bias into the obtained results. Therefore, further investigation using a larger sample size and a multicenter design is warranted to enhance the robustness and generalizability of these findings.

5. Conclusions

In conclusion, multimodal ultrasound offers valuable insights into breast cancer lesions, aiding in the assessment of NAC efficacy. Notably, tumor diameter, PI and AUC in multimodal ultrasound were identified as more effective predictors of NAC outcomes. Collectively, these results highlight the potential of multimodal ultrasound as a valuable tool in managing breast cancer patients undergoing NAC.

AVAILABILITY OF DATA AND MATERIALS

The authors declare that all data supporting the findings of this study are available within the paper and any raw data can be obtained from the corresponding author upon request.

AUTHOR CONTRIBUTIONS

XQH and TS—designed the study and carried them out, prepared the manuscript for publication and reviewed the draft of the manuscript. XQH, JXG, YBL, WH, ZML—supervised the data collection, analyzed the data, interpreted the data. All authors have read and approved the manuscript.

ETHICS APPROVAL AND CONSENT TO PARTICIPATE

Ethical approval was obtained from the Ethics Committee of the First Affiliated Hospital of Xinjiang Medical University (Ethics Approval Number: K202310-02). Written informed consent was obtained from a legally authorized representative(s) for anonymized patient information to be published in this article.

ACKNOWLEDGMENT

Not applicable.

FUNDING

This work was supported by Natural Youth Science Foundation of Xinjiang Uygur Autonomous Region (Grant No. 2022D01C772).

CONFLICT OF INTEREST

The authors declare no conflict of interest.

REFERENCES

[1] Korde LA, Somerfield MR, Carey LA, Crews JR, Denduluri N, Hwang ES, *et al*. Neoadjuvant chemotherapy, endocrine therapy, and targeted therapy for breast cancer: ASCO guideline. Journal of Clinical Oncology. 2021; 39: 1485–1505.

[2] Martin M, Hegg R, Kim SB, Schenker M, Grecea D, Garcia-Saenz JA, *et al*. Treatment with adjuvant abemaciclib plus endocrine therapy in patients with high-risk early breast cancer who received neoadjuvant chemotherapy: a prespecified analysis of the monarche randomized clinical trial. JAMA Oncology. 2022; 8: 1190–1194.

[3] Ofri A, Elstner K, Mann G, Kumar S, Warrier S. Neoadjuvant chemotherapy in non-metastatic breast cancer: the surgeon's perspective. The Surgeon. 2023; 21: 356–360.

[4] Kerr AJ, Dodwell D, McGale P, Holt F, Duane F, Mannu G, *et al*. Adjuvant and neoadjuvant breast cancer treatments: a systematic review of their effects on mortality. Cancer Treatment Reviews. 2022; 105: 102375.

[5] Fisher CS. Neoadjuvant chemotherapy for breast cancer: the ultimate "Spy". Annals of Surgical Oncology. 2022; 29: 6508–6510.

[6] Dieci MV, Guarneri V, Tosi A, Bisagni G, Musolino A, Spazzapan S, *et al*. Neoadjuvant chemotherapy and immunotherapy in luminal b-like breast cancer: results of the phase II GIADA trial. Clinical Cancer Research. 2022; 28: 308–317.

[7] Zhou BY, Wang LF, Yin HH, Wu TF, Ren TT, Peng C, *et al*. Decoding the molecular subtypes of breast cancer seen on multimodal ultrasound images using an assembled convolutional neural network model: a prospective and multicentre study. EBioMedicine. 2021; 74: 103684.

[8] Xu Z, Wang Y, Chen M, Zhang Q. Multi-region radiomics for artificially intelligent diagnosis of breast cancer using multimodal ultrasound. Computers in Biology and Medicine. 2022; 149: 105920.

[9] Kawiak A, Kostecka A. Regulation of Bcl-2 family proteins in estrogen receptor-positive breast cancer and their implications in endocrine therapy. Cancers. 2022; 14: 279.

[10] Coffey K, Jochelson MS. Contrast-enhanced mammography in breast cancer screening. European Journal of Radiology. 2022; 156: 110513.

[11] Bian J, Zhang J, Hou X. Diagnostic accuracy of ultrasound shear wave elastography combined with superb microvascular imaging for breast tumors: a protocol for systematic review and meta-analysis. Medicine. 2021; 100: e26262.

[12] Zhang G, Xu Z, Yu M, Gao H. Bcl-2 interacting protein 3 (BNIP3) promotes tumor growth in breast cancer under hypoxic conditions through an autophagy-dependent pathway. Bioengineered. 2022; 13: 6280–6292.

[13] Kuerer HM, Smith BD, Krishnamurthy S, Yang WT, Valero V, Shen Y, *et al*. Eliminating breast surgery for invasive breast cancer in exceptional responders to neoadjuvant systemic therapy: a multicentre, single-arm, phase 2 trial. The Lancet Oncology. 2022; 23: 1517–1524.

[14] Provenzano E. Neoadjuvant chemotherapy for breast cancer: moving beyond pathological complete response in the molecular age. Acta Medica Academica. 2021; 50: 88–109.

[15] Tarantino P, Gandini S, Trapani D, Criscitiello C, Curigliano G. Immunotherapy addition to neoadjuvant chemotherapy for early triple negative breast cancer: a systematic review and meta-analysis of randomized clinical trials. Critical Reviews in Oncology/Hematology. 2021; 159: 103223.

[16] See SHC, Siziopikou KP. Pathologic evaluation of specimens after neoadjuvant chemotherapy in breast cancer: current recommendations and challenges. Pathology—Research and Practice. 2022; 230: 153753.

[17] Jin J, Liu YH, Zhang B. Diagnostic performance of strain and shear wave elastography for the response to neoadjuvant chemotherapy in breast cancer patients: systematic review and meta-analysis. Journal of Ultrasound in Medicine. 2022; 41: 2459–2466.

[18] Liu Y, Wang Y, Wang Y, Xie Y, Cui Y, Feng S, *et al*. Early

prediction of treatment response to neoadjuvant chemotherapy based on longitudinal ultrasound images of HER2-positive breast cancer patients by Siamese multi-task network: a multicentre, retrospective cohort study. EClinicalMedicine. 2022; 52: 101562.

[19] Wang S, Wen W, Zhao H, Liu J, Wan X, Lan Z, *et al*. Prediction of clinical response to neoadjuvant therapy in advanced breast cancer by baseline B-mode ultrasound, shear-wave elastography, and pathological information. Frontiers in Oncology. 2023; 13: 1096571.

[20] Rix A, Piepenbrock M, Flege B, von Stillfried S, Koczera P, Opacic T, *et al*. Effects of contrast-enhanced ultrasound treatment on neoadjuvant chemotherapy in breast cancer. Theranostics. 2021; 11: 9557–9570.

[21] Hayashi M, Yamamoto Y, Iwase H. Clinical imaging for the prediction of neoadjuvant chemotherapy response in breast cancer. Chinese Clinical Oncology. 2020; 9: 31.

[22] Zheng A, Zhang L, Song X, Jin F. Clinical significance of SPRY4-IT1 in efficacy and survival prediction in breast cancer patients undergoing neoadjuvant chemotherapy. Histology & Histopathology. 2020; 35: 361–370.

[23] Guo J, Wang BH, He M, Fu P, Yao M, Jiang T. Contrast-enhanced ultrasonography for early prediction of response of neoadjuvant chemotherapy in breast cancer. Frontiers in Oncology. 2022; 12: 1026647.

[24] Sharma A, Grover SB, Mani C, Ahluwalia C. Contrast enhanced ultrasound quantitative parameters for assessing neoadjuvant chemotherapy response in patients with locally advanced breast cancer. The British Journal of Radiology. 2021; 94: 20201160.

[25] Li C, Yao M, Li X, Shao S, Chen J, Li G, *et al*. Ultrasonic multimodality imaging features and the classification value of nonpuerperal mastitis. Journal of Clinical Ultrasound. 2022; 50: 675–684.

[26] Kanakaveti V, Ramasamy S, Kanumuri R, Balasubramanian V, Saravanan R, Ezhil I, *et al*. Novel BH4-BCL-2 domain antagonists induce BCL-2-mediated apoptosis in triple-negative breast cancer. Cancers. 2022; 14: 5241.

[27] Al-Zubaidy HFS, Majeed SR, Al-Koofee DAF. Evaluation of bax and BCL 2 genes polymorphisms in Iraqi women with breast cancer. Archives of Razi Institute. 2022; 77: 799–808.

[28] Ozoran E, Trabulus FDC, Erhan D, Batar B, Guven M. Association of XRCC3, XRCC4, BAX, and BCL-2 polymorphisms with the risk of breast cancer. International Journal of Breast Cancer. 2022; 2022: 5817841.

[29] Turk M, Tatli O, Alkan HF, Ozfiliz Kilbas P, Alkurt G, Dinler Doganay G. Co-chaperone Bag-1 plays a role in the autophagy-dependent cell survival through Beclin 1 interaction. Molecules. 2021; 26: 854.

[30] Chen X, He C, Han D, Zhou M, Wang Q, Tian J, *et al*. The predictive value of Ki-67 before neoadjuvant chemotherapy for breast cancer: a systematic review and meta-analysis. Future Oncology. 2017; 13: 843–857.

[31] Kim JY, Oh JM, Lee SK, Yu J, Lee JE, Kim SW, *et al*. Improved prediction of survival outcomes using residual cancer burden in combination with Ki-67 in breast cancer patients underwent neoadjuvant chemotherapy. Frontiers in Oncology. 2022; 12: 903372.

How to cite this article: Xueqin Hou, Junxi Gao, Yibin Liu, Wei Han, Zhiming Li, Tao Song. Predictive value of multimodal ultrasound imaging and BCL-2 expression levels in the outcome of neoadjuvant chemotherapy for breast cancer. European Journal of Gynaecological Oncology. 2024; 45(2): 16-23. doi: 10.22514/ejgo.2024.023.